

THERMODYNAMIC VARIABLES FROM SPECTATOR DE- CAY*

W. Trautmann¹ for the ALADIN collaboration²

¹Gesellschaft für Schwerionenforschung mbH
D-64291 Darmstadt
Germany

²Catania, Darmstadt, East Lansing, Frankfurt,
Milano, Moscow, Rossendorf, Warsaw

INTRODUCTION

The Van-der-Waals-type range dependence of the nuclear forces has provided a good part of the motivation for fragmentation studies. The predictions of a liquid-gas phase transition in nuclear matter [1, 2] have raised the hope that signals of it may be identified in reactions of finite nuclei. The observation of multifragmentation [3, 4, 5] represented a major breakthrough in this direction, as it indicated that the created nuclear systems may actually pass through states of high temperature and low density during the later stages of the reaction. Multifragmentation has been predicted [6, 7] to be the dominant decay mode under such conditions that are similar to those expected for the coexistence region in the nuclear-matter phase diagram.

Many features of multifragmentation are well reproduced by the statistical multifragmentation models [6, 7, 8]. They predominantly include the fragment distributions and correlations describing the populated partition space. But also kinetic observables such as the energies or velocity correlations of the produced fragments have been found to agree with the statistical predictions in certain cases [9, 10]. The essential assumption on which these models are based is that of a single equilibrated breakup state at the end of the dynamical evolution and of a statistical population of the corresponding phase space. To the extent that it is realized in nature, this scenario offers the possibility to map out the nuclear phase diagram, even though for finite nuclei, by sampling the thermodynamic equilibrium conditions associated with the multi-fragment breakup channels.

Considerable progress has been made with this program during recent years. Multifragmentation has been studied over a wide range of different classes of high-

* presented at 14th Winter Workshop on Nuclear Dynamics, Snowbird, Utah, 31 Jan - 7 Feb 1998

energy reactions and breakup temperatures have been deduced from the measured data. The correlation of the temperature with the excitation energy, often referred to as the caloric curve of nuclei and first reported for spectator decays following $^{197}\text{Au} + ^{197}\text{Au}$ reactions at 600 MeV per nucleon [11], has also been derived for other cases [10, 12, 13]. Critical evaluations of the obtained results and of the applied methods have followed. More work is clearly needed in order to complete the picture [14].

In this contribution, the focus will be on the decay of excited spectator nuclei [15]. New results will be reported that were obtained in two recent experiments with the ALADIN spectrometer at SIS in which reactions of ^{197}Au on ^{197}Au in the regime of relativistic energies up to 1 GeV per nucleon were studied. In the first experiment, the ALADIN spectrometer was used to detect and identify the products of the projectile-spectator decay [16]. The Large-Area Neutron Detector (LAND) was used to measure coincident free neutrons emitted by the projectile source. In the second experiment, three multi-detector hodoscopes, consisting of a total of 216 Si-CsI(Tl) telescopes, and three high-resolution telescopes were positioned at backward angles to measure the yields and correlations of isotopically resolved light fragments of the target-spectator decay [17]. From these data excitation energies and masses, temperatures, and densities were deduced. Before proceeding to the discussion of these new data some of the indications for equilibration during the spectator decay will be briefly recalled.

EVIDENCE FOR EQUILIBRATION

The universal features of the spectator decay, as apparent in the observed Z_{bound} scaling of the measured charge correlations, were the first and perhaps most striking indications for equilibrium [16]. The quantity Z_{bound} is defined as the sum of the atomic numbers Z_i of all projectile fragments with $Z_i \geq 2$. It represents the charge of the original spectator system reduced by the number of hydrogen isotopes emitted during its decay.

The invariance of the fragmentation patterns, when plotted as a function of Z_{bound} , suggests that the memory of the entrance channel and of the dynamics governing the primary interaction of the colliding nuclei is lost. This feature extends to other observables. The transverse-momentum widths of the fragments, as shown in Fig. 1, do not change with the bombarding energy, indicating that collective contributions to the transverse motion are small. The equilibration of the three kinetic degrees

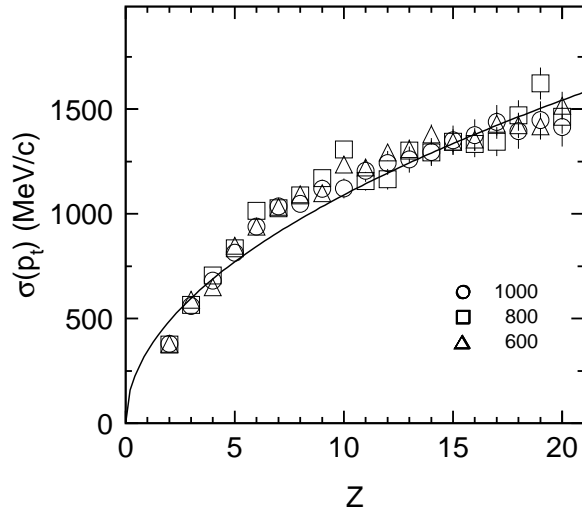


Figure 1: Widths of the transverse-momentum distributions $\sigma(p_t)$ as a function of the fragment atomic number Z for the reactions ^{197}Au on ^{197}Au at $E/A = 600, 800,$ and 1000 MeV and for $20 \leq Z_{\text{bound}} \leq 60$. The line is proportional to \sqrt{Z} (from Ref. [16]).

of freedom in the moving frame of the projectile spectator was confirmed by the analysis of the measured velocity spectra [16]. The square-root dependence on the atomic number Z implies kinetic energies nearly independent of Z and hence of the mass.

The success of the statistical multifragmentation model in describing the observed population of the partition space may be seen as a further argument for equilibration. Here the main task consists of finding an appropriate ensemble of excited nuclei to be subjected to the multi-fragment decay according to the model prescription. Starting from the entrance channel may not necessarily provide sufficiently realistic ensembles, even though a good description of the fragment correlations was obtained with the quantum-molecular-dynamics model coupled to the statistical multifragmentation model [18]. An alternative method consists of using empirically derived ensembles. Near perfect descriptions of the measured correlations, including their dispersions around the mean behaviour, can be achieved [8, 17]. The mathematical procedure of backtracing allows for studying the uniqueness of the obtained solutions and their sensitivities to the observables that were used to generate it [19].

The ensemble derived empirically for the reaction ^{197}Au on ^{197}Au at 1000 MeV per nucleon is shown in Fig. 2. Its capability of reproducing the measured mean multiplicity of intermediate-mass fragments and the mean charge asymmetry of the

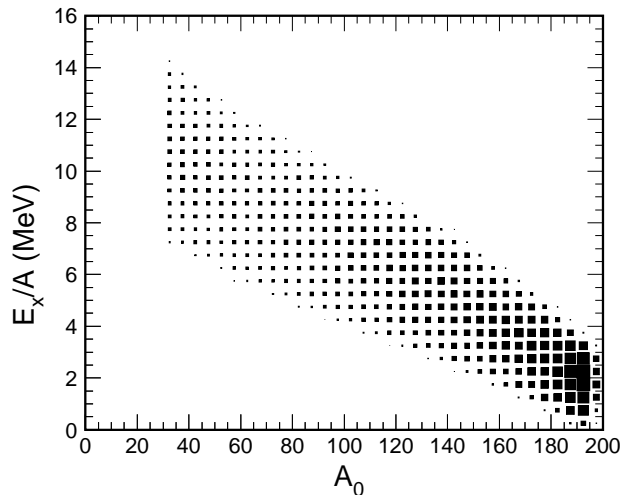


Figure 2: Excitation energy E_x/A as a function of the mass A_0 for the ensemble of excited spectator nuclei used as input for the calculations with the statistical multifragmentation model. The area of the squares is proportional to the intensity (from Ref. [17]).

two heaviest fragments is illustrated in Fig. 3 where the dashed and dotted lines show the model results for E_x/A chosen 15% above and below the adopted values. In the region $Z_{bound} > 30$, the mean excitation energy of the ensemble of spectator nuclei was found to be well constrained by the mean fragment multiplicity alone. At $Z_{bound} \approx 30$ and below, the charge asymmetry was a necessary second constraint while, at the lowest values of Z_{bound} , neither the multiplicity nor the asymmetry provided rigid constraints on the excitation energy.

The spectator source, well localized in rapidity [16] and, apparently, exhibiting so many signs of equilibration, seems an excellent candidate for studying the nuclear phase diagram. Dynamical studies also support this conclusion [20, 21]. There are limitations, however, which are mainly seen in the emission of nucleons and very light particles. Here the components from reaction stages that lead to the formation of the spectator system and from its subsequent breakup overlap, thereby creating difficulties for the extraction of the equilibrium properties. This is particularly apparent in the case of the excitation energy which will be discussed in the next section.

EXCITATION ENERGY

A method to determine the excitation energy from the experimental data was first presented by Campi *et al.* [22] and applied to the earlier $^{197}\text{Au} + \text{Cu}$ data

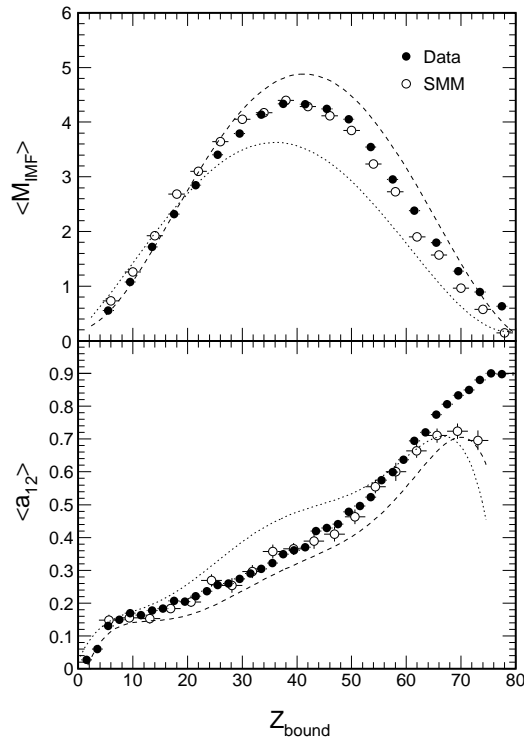


Figure 3: Mean multiplicity of intermediate-mass fragments $\langle M_{IMF} \rangle$ (top) and mean charge asymmetry $\langle a_{12} \rangle$ (bottom) as a function of Z_{bound} , as obtained from the calculations with the statistical multifragmentation model (open circles), in comparison to the experimental data for ^{197}Au on ^{197}Au at $E/A = 1000$ MeV (dots, from Ref. [16]). The dashed and dotted lines show the results of the calculations with excitation energies E_x/A 15% above and 15% below the adopted values, respectively. Note that the trigger threshold affected the data of Ref. [16] at $Z_{bound} \geq 65$ (from Ref. [17]).

[23]. It is based on the idea of calorimetry which requires a complete knowledge of all decay products, including their atomic numbers, masses, and kinetic energies. In this work, the measured abundances for $Z \geq 2$ were used and, e.g., the yields of hydrogen isotopes were deduced by extrapolating to $Z = 1$. In the same type of analysis with the more recent data for $^{197}\text{Au} + ^{197}\text{Au}$ at 600 MeV per nucleon, the data on neutron production measured with LAND were taken into account [11]. Since the hydrogen isotopes were not detected assumptions concerning the overall N/Z ratio of the spectator, the intensity ratio of protons, deuterons, and tritons, and the kinetic energies of hydrogen isotopes had to be made.

The latest evaluation of the excitation energy included the measured neutron data for three bombarding energies and the data for hydrogen emission from the target spectator at 1000 MeV per nucleon [24]. For the case of 600 MeV per nucleon, the

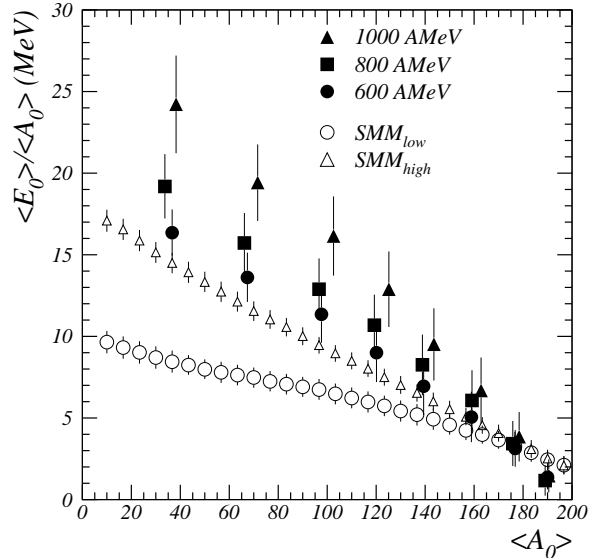


Figure 4: Mean excitation energy per nucleon $\langle E_0 \rangle / \langle A_0 \rangle$ as a function of the spectator mass $\langle A_0 \rangle$ for the reaction ^{197}Au on ^{197}Au at three bombarding energies as indicated. The open symbols denote the upper and lower limit of the mean excitation energy that may be derived from analyses with the statistical multifragmentation model (from Ref. [24]).

difference to the published energy values [11] amounted to about 10%. More importantly, however, the deduced spectator energy was found to depend considerably on the bombarding energy (Fig. 4). It increases by about 30% over the range 600 to 1000 MeV per nucleon which is in contrast to the universality observed for other observables (previous section). The origin of this rise lies solely in the behavior of the mean kinetic energies of neutrons in the spectator frame (Fig. 5). They have a large effect on the deduced total excitation energy, first, because the neutron multiplicity is large and, second, because the hydrogen isotopes, measured only at 1000 MeV per nucleon, were assumed to scale in the same way as the neutrons do.

It is obvious that this uncertainty represents a considerable problem, a memory of the entrance channel is inconsistent with the idea of measuring thermodynamic properties of an equilibrated breakup state. It is reasonable to assume that part of the experimentally determined energy may be due to pre-equilibrium or pre-breakup emission, even though the analysis of nucleon emission is restricted to the data at forward (backward) angles in the projectile (target) frame (Fig. 6). The experimental excitation energies are larger than the range of energies potentially consistent with the statistical multifragmentation model (Fig. 4), and the spectra of hydrogen iso-

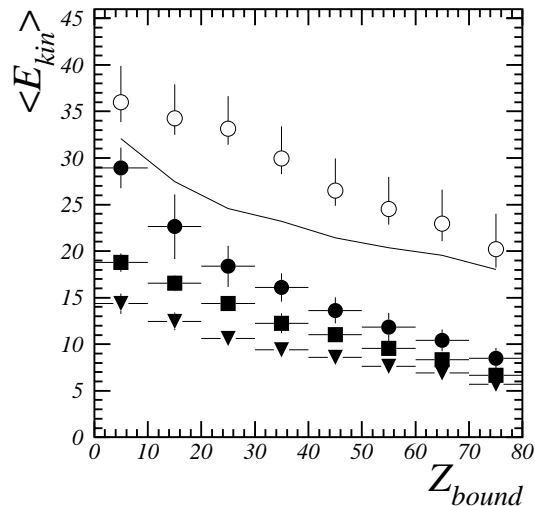


Figure 5: Mean kinetic energy of neutrons (full symbols) in the rest frame of the projectile spectator as obtained in measurements including LAND for the reaction ^{197}Au on ^{197}Au at $E/A = 600$ (triangles), 800 (squares), and 1000 MeV (circles). For $E/A = 1000$ MeV, the measured mean kinetic energies of protons (open circles) are shown in comparison to the sum of the neutron kinetic energies and an estimated Coulomb contribution (full line, from Ref. [24]).

topes, measured with the high-resolution telescopes, exhibit yields and slopes much larger than predicted by the model [17]. The process of spectator formation involves secondary scatterings of fireball nucleons on spectator matter which may generate a pre-breakup source centered close to the spectator rapidity. Experimentally, the next step should consist of complementing the neutron data with equivalent data for proton and light-charged-particle emission at several bombarding energies.

TEMPERATURE

The shape of the caloric curve [11], reminiscent of first-order phase transitions in ordinary liquids, and its similarity to predictions of microscopic statistical models [6, 7, 17], has initiated a widespread discussion of whether nuclear temperatures of this magnitude can be measured reliably (see Refs. [25, 26] and references given in these recent papers) and whether this observation may indeed be linked to a transition towards the vapor phase [27, 28].

Here we restrict ourselves to new results obtained from the study of the target spectator at backward angles in the laboratory in $^{197}\text{Au} + ^{197}\text{Au}$ collisions at 1000

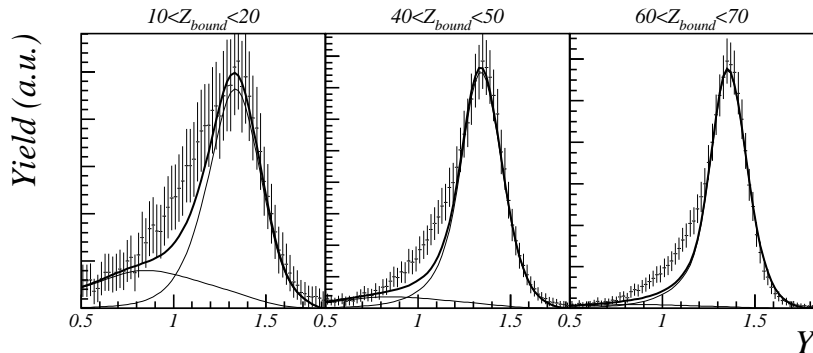


Figure 6: Rapidity spectra of neutrons measured with LAND for three bins in Z_{bound} for the reaction ^{197}Au on ^{197}Au at $E/A = 1000$ MeV and a cut in transverse momentum of $35 \text{ MeV}/c \leq p_t \leq 70 \text{ MeV}/c$. The thick lines represent the result of fits assuming a projectile and a mid-rapidity source. The individual contributions of these sources are given by the thin lines (from Ref. [24]).

MeV per nucleon. From the isotopically resolved yields of hydrogen, helium, and lithium isotopes breakup temperatures T_{HeLi} , T_{HePd} , and T_{HeDt} were derived [29]. The corrections for sequential feeding of the ground-state yields, based on calculations with the quantum statistical model [30], resulted in good qualitative agreement for the three temperature observables [17].

The corrected temperature T_{HeLi} is shown in Fig. 7. With decreasing Z_{bound} , it increases from $T = 4$ MeV for peripheral collisions to about 10 MeV for the most central collisions. Within the errors, these values are in good agreement with those measured for projectile spectators in the same reaction at 600 MeV per nucleon. In both cases, the displayed data symbols represent the mean values of the range of systematic uncertainties associated with the two different experiments while the errors include both statistical and systematic contributions. The projectile temperatures are the result of a new analysis of the original data and are somewhat higher, between 10% and 20%, than those reported previously [11]. Their larger errors follow from a reassessment of the potential ^4He contamination of the ^6Li yield caused by Z misidentification. The invariance of the breakup temperature with the bombarding energy is consistent with the observed universality of the spectator decay.

Calculations with the statistical multifragmentation model were performed for the ensemble of excited spectator nuclei shown in Fig. 2. Results have already been shown in Fig. 3. The solid line in Fig. 7 represents the thermodynamic temperature

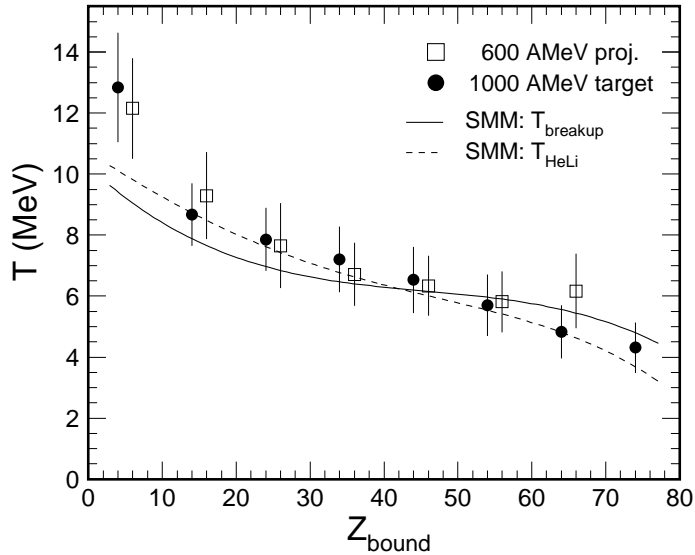


Figure 7: Temperatures T_{HeLi} of the target spectator for the reaction ^{197}Au on ^{197}Au at $E/A = 1000$ MeV (dots) and of the projectile spectator at $E/A = 600$ MeV (open squares) as a function of Z_{bound} . The data symbols represent averages over bins of 10-units width and, for clarity, are laterally displaced by 1 unit of Z_{bound} . Statistical and systematic contributions are included in the displayed errors. The lines are smoothed fit curves describing the breakup temperature $T_{breakup}$ (full line) and the isotopic temperature T_{HeLi} (dashed line) calculated with the statistical multifragmentation model (from Ref. [17]).

T obtained in these calculations. With decreasing Z_{bound} , it increases monotonically from about 5 to 9 MeV. Over a wide range of Z_{bound} it remains close to $T = 6$ MeV which reflects the plateau predicted by the statistical multifragmentation model for the range of excitation energies $3 \text{ MeV} \leq E_x/A \leq 10 \text{ MeV}$ [7]. In model calculations performed for a fixed spectator mass, the plateau is associated with a strong and monotonic rise of the fragment multiplicities. Experimentally, due to the decrease of the spectator mass with increasing excitation energy (Fig. 2), the production of intermediate-mass fragments passes through a maximum in the corresponding range of Z_{bound} from about 20 to 60 (Fig. 3).

The dashed line gives the temperature T_{HeLi} obtained from the calculated isotope yields. Because of sequential feeding, it differs from the thermodynamic temperature, the uncorrected temperature $T_{\text{HeLi},0}$ being somewhat lower. Here, in order to permit the direct comparison with the experimental data in one figure, we display T_{HeLi} which has been corrected in the same way with the factor 1.2 suggested by the

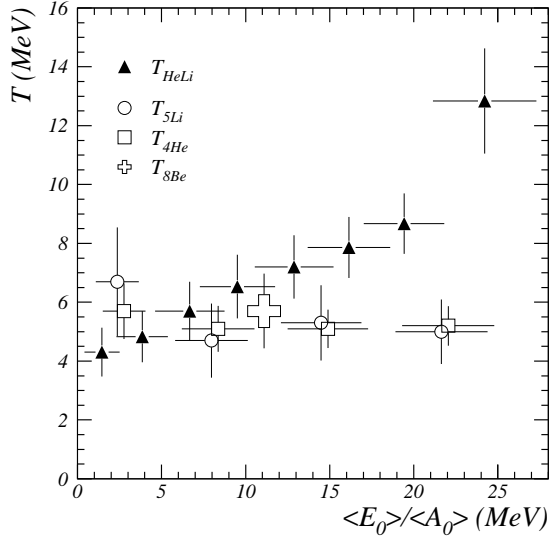


Figure 8: Measured isotope temperature T_{HeLi} (full triangles) and excited-state temperatures (open symbols) as a function of the experimental excitation energy per nucleon $\langle E_0 \rangle / \langle A_0 \rangle$ for the reaction ^{197}Au on ^{197}Au at $E/A = 1000$ MeV. The indicated uncertainties are mainly of systematic origin. The displayed value of T_{8Be} represents an average over the full range of $\langle E_0 \rangle / \langle A_0 \rangle$ (from Ref. [24]).

quantum statistical model. The calculated T_{HeLi} exhibits a more continuous rise with decreasing Z_{bound} than the thermodynamic temperature and is in very good agreement with the measured values. We thus find that, with the parameters needed to reproduce the observed charge partitions, this temperature-sensitive observable is well reproduced. A necessary requirement for a consistent statistical description of the spectator fragmentation is thus fulfilled.

In the same experiment excited-state temperatures [31, 32] were determined from the populations of particle-unstable resonances measured with the Si-CsI hodoscopes. The peak structures were identified by using the technique of correlation functions, and background corrections were based on results obtained for resonance-free pairs of fragments with $Z \leq 3$, such as p-d, d-d, up to ^3He - ^7Li . Correlated yields of p-t, p- ^4He , d- ^3He , ^4He - ^4He , and p- ^7Li coincidences and ^4He singles yields were used to deduce temperatures from the populations of states in ^4He (g.s.; group of three states at 20.21 MeV and higher), ^5Li (g.s.; 16.66 MeV), and ^8Be (3.04 MeV; group of five states at 17.64 MeV and higher). The probabilities for the coincident detection of the decay products of these resonances were calculated with a Monte-Carlo model

[32, 33]. The uncertainty of the background subtraction is the main contribution to the errors of the deduced temperatures.

The values for the three excited-state temperatures are given in Fig. 8 as a function of the experimental excitation energy $\langle E_0 \rangle / \langle A_0 \rangle$. Mutually consistent with each other, they appear to be virtually independent of the excitation energy, centering about a mean value of ≈ 5 MeV. This is in striking contrast to the monotonically rising isotope temperature T_{HeLi} which is shown in comparison.

A saturation of excited-state temperatures and a similar difference to the behavior of isotope temperatures has also been observed in central $^{197}\text{Au} + ^{197}\text{Au}$ collisions at incident energies $E/A = 50$ MeV to 200 MeV [34]. The interpretation given there starts from the fact that the excited states used for the temperature evaluation are very specific quantum states which may not exist in the nuclear medium in identical forms [35, 36, 37]. The observed asymptotic states can develop and survive only at very low densities that may not be reached before the cluster is emitted into vacuum. Accordingly, the excited-state populations should reflect the temperature and its fluctuations at this final stage of fragment emission. The obtained mean value near 5 MeV is not inconsistent with results of dynamical calculations based on the BUU model [20].

DENSITY

Expansion is a basic conceptual feature of both the statistical multifragmentation and the liquid-gas phase transition. A volume of about six to eight times that occupied at saturation density is assumed in the statistical multifragmentation models while the critical volume in the case of infinite nuclear matter has about three times the saturation value. The experimental confirmation of expansion or low breakup density is therefore of the highest significance.

In central collisions of heavy nuclei, expansion is evident from the observation of radial collective flow [38]. Significant radial flow is not observed in spectator decays, and evidence for expansion has been obtained, indirectly, from model comparisons. Models that assume sequential emission from the surfaces of nuclear systems at saturation density underpredict the fragment multiplicities while those assuming expanded breakup volumes yield satisfactory descriptions of the populated partition space [39]. The disappearance of the Coulomb peaks in the kinetic-energy spectra of emitted light particles and fragments, associated with increasing fragment produc-

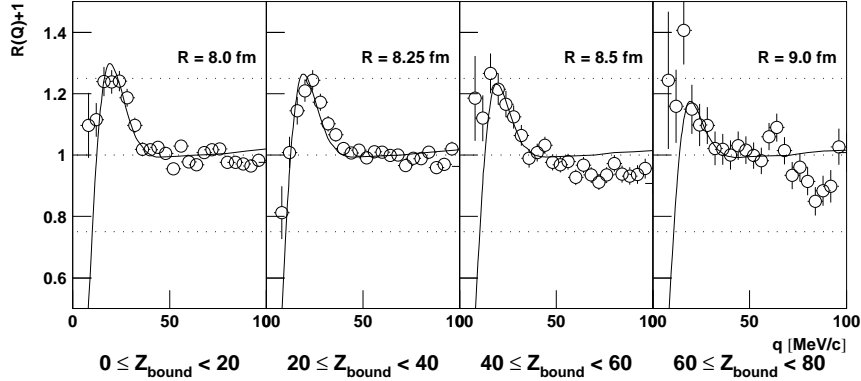


Figure 9: Proton-proton correlation functions for the indicated intervals of Z_{bound} , measured at $\Theta_{lab} \approx 135^\circ$ for the reaction ^{197}Au on ^{197}Au at $E/A = 1000$ MeV. The full lines are obtained from the analysis with the Koonin-Pratt formalism, the resulting source radii are indicated (from Ref. [42]).

tion, provides additional evidence consistent with volume emission or emission from expanded systems [40].

Interferometric methods permit experimental determinations of the breakup volume or, more precisely, of the space-time extension of where the emitted products had suffered their last collision [41]. In the present case of spectator decay at relativistic energies the time scales should be rather short and the data, in good approximation, may be directly related to the breakup volume that is of interest here.

Proton-proton correlation functions measured at angles of $\Theta_{lab} \approx 135^\circ$ are shown in Fig. 9. They are characterized by a depression at small relative momenta, caused by Coulomb repulsion, and by a peak near $q = 20$ MeV/c that is caused by the S-wave nuclear interaction. Its comparatively small amplitude signals a large spatial extension of the proton source. The quantitative analysis of these data was performed with the Koonin-Pratt formalism [43]. A uniform sphere was assumed for the proton source. The deduced radii are of the order of 8 to 9 fm which is distinctly larger than the radius of 6.5 to 7 fm of a gold nucleus at normal density. The structure of the correlation functions is somewhat obscured at larger Z_{bound} but there is no indication that the radii and thus the volume should significantly change with impact parameter. The derived density, however, decreases considerably with increasing centrality, caused by the changing number of spectator constituents A_0 (Fig. 10). These spectator masses result from the calorimetric analysis described

above and are found to be in good agreement with the prediction of the geometric participant-spectator model [44]. The mean relative density decreases to values below $\rho/\rho_0 = 0.2$ for the most central bin, i.e. smallest Z_{bound} . The deduced values as well as the variation with centrality compare well with the densities entering the statistical multifragmentation model in the version that uses a fixed cracking distance for the placement of fragments inside the breakup volume [7]. We recall here that the proton multiplicities and kinetic-energy spectra indicate a predominantly pre-breakup emission. This does not necessarily exclude the possibility that their interaction with the forming spectator matter causes the interferometric picture to reflect the extension of the latter.

Besides the proton-proton correlations also correlations of other light charged particles were used to determine breakup radii. Pronounced resonances are exhibited by the p- α (^5Li , g.s.), d- α (^6Li , 2.19 MeV), and t- α (^7Li , 4.63 MeV) correlation functions. Their peak heights were analyzed using the numerical results of Boal and Shillcock [45]. The deduced values, within errors are in qualitative agreement with the proton values. Their much smaller error bars demonstrate that higher accuracies may be reached with these pronounced resonances of particle unbound states in light nuclei. The further development of the formalism needed for their quantitative interpretation seems therefore highly desirable.

SUMMARY AND PERSPECTIVES

New results for the mass, excitation energy, temperature, and density of excited spectator systems at breakup have been presented. The discussion of these data was meant to demonstrate that methods exist to determine these thermodynamic variables from the experiment. It was also intended to show that they are not without problems and that, perhaps, serious conceptual difficulties exist which may make it very difficult to arrive at unambiguous results. The problem caused for the excitation energy by the dynamical process of spectator formation is an example.

It should be rewarding to further pursue this program, not only because of the hope to better identify signals of the liquid-gas phase transition but also because unexpected results may appear, as demonstrated for the temperatures. The saturation of the excited-state temperatures, according to the interpretation given here, is an interesting in-medium effect in itself. It also has the consequence that it may provide us with a means to determine rather reliably the internal temperatures of fragments

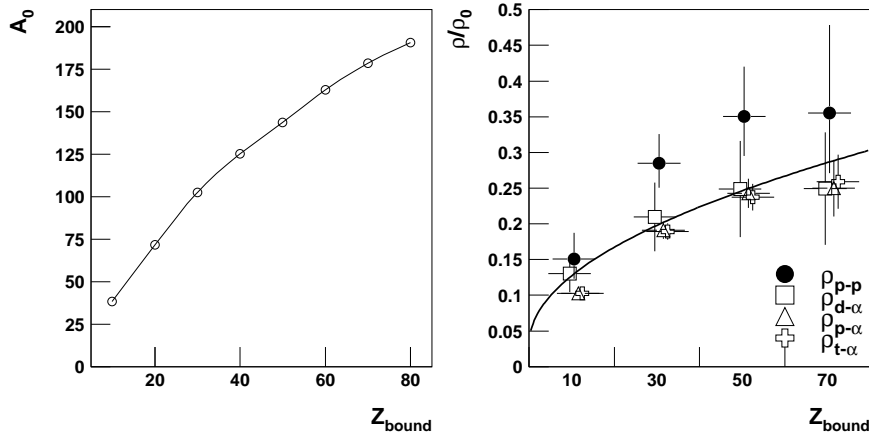


Figure 10: Spectator mass $\langle A_0 \rangle$ (left panel) and relative density ρ/ρ_0 (right panel) as a function of Z_{bound} for the reaction ^{197}Au on ^{197}Au at $E/A = 1000$ MeV. The lines are meant to guide the eye. The densities were derived from proton-proton correlations (Fig. 9) and from correlation functions constructed for light charged particles as indicated (open symbols, from Ref. [42]).

at their final separation from the system.

The interferometry with light charged particles confirms the low density of the breakup configuration. For more precise evaluations the formalisms needed to deduce radii and densities from interferometric measurements will need continuing development. Measurements of radii for different fragment species, possibly emitted at different stages of the reaction, may allow us to test and refine the otherwise so successful picture of the single breakup state in the spectator decay.

References

- [1] H. Jaqaman *et al.*, *Phys. Rev. C* 27:2782 (1983).
- [2] D.K. Scott, *Proceedings of the 6th High Energy Heavy Ion Study*, Berkeley (1983), ed. H.G. Pugh *et al.*, report LBL-16281, p. 263.
- [3] B. Jakobsson *et al.*, *Z. Phys. A* 307:293 (1982).
- [4] E.M. Friedlander *et al.*, *Phys. Rev. C* 27:2436 (1983).
- [5] For a recent review see L.G. Moretto and G.J. Wozniak, *Ann. Rev. Nucl. Part. Science* 43:379 (1993).
- [6] D.H.E. Gross, *Rep. Prog. Phys.* 53:605 (1990).
- [7] J.P. Bondorf *et al.*, *Phys. Rep.* 257:133 (1995).

- [8] A.S. Botvina *et al.*, *Nucl. Phys. A* 584:737 (1995).
- [9] Bao-An Li *et al.*, *Phys. Lett. B* 335:1 (1994).
- [10] K. Kwiatkowski *et al.*, *Proceedings of the XXXV International Winter Meeting on Nuclear Physics*, Bormio (1997), ed. I. Iori (Ricerca Scientifica ed Educazione Permanente, Milano, 1997), p. 432.
- [11] J. Pochodzalla *et al.*, *Phys. Rev. Lett.* 75:1040 (1995).
- [12] J.A. Hauger *et al.*, *Phys. Rev. Lett.* 77:235 (1996).
- [13] Y.-G. Ma *et al.*, *Phys. Lett. B* 390:41 (1997).
- [14] For a more comprehensive status report see J. Pochodzalla, *Prog. Part. Nucl. Phys.* 39:443 (1997).
- [15] W. Trautmann, Multifragmentation in relativistic heavy-ion reactions, *in*: "Correlations and Clustering Phenomena in Subatomic Physics," M.N. Harakeh, J.H. Koch, and O. Scholten, ed., Plenum Press, New York (1997).
- [16] A. Schüttauf *et al.*, *Nucl. Phys. A* 607:457 (1996).
- [17] Hongfei Xi *et al.*, *Z. Phys. A* 359:397 (1997).
- [18] J. Konopka *et al.*, *Prog. Part. Nucl. Phys.* 30:301 (1993).
- [19] P. Désesquelles *et al.*, *Nucl. Phys. A* 604:183 (1996).
- [20] C. Fuchs *et al.*, *Nucl. Phys. A* 626:987 (1997).
- [21] P.-B. Gossiaux and J. Aichelin, *Phys. Rev. C* 56:2109 (1997).
- [22] X. Campi *et al.*, *Phys. Rev. C* 50:R2680 (1994).
- [23] P. Kreuzt *et al.*, *Nucl. Phys. A* 556:672 (1993).
- [24] C. Groß, PhD thesis, Universität Frankfurt (1998).
- [25] Hongfei Xi *et al.*, *Phys. Rev. C* 54:R2163 (1996).
- [26] F. Gulminelli and D. Durand, *Nucl. Phys. A* 615:117 (1997).
- [27] J.B. Natowitz *et al.*, *Phys. Rev. C* 52:R2322 (1995).
- [28] L.G. Moretto *et al.*, *Phys. Rev. Lett.* 76:2822 (1996).
- [29] S. Albergo *et al.*, *Il Nuovo Cimento* 89 A:1 (1985).
- [30] J. Konopka *et al.*, *Phys. Rev. C* 50:2085 (1994).
- [31] J. Pochodzalla *et al.*, *Phys. Rev. C* 35:1695 (1987).
- [32] G.J. Kunde *et al.*, *Phys. Lett. B* 272:202 (1991).
- [33] V. Serfling, PhD thesis, Universität Frankfurt (1997).

- [34] V. Serfling *et al.*, *Phys. Rev. Lett.* (1998), in press.
- [35] P. Danielewicz and Q. Pan, *Phys. Rev. C* 46:2002 (1992).
- [36] M. Schmidt *et al.*, *Ann. Phys. (N.Y.)* 202:57 (1990).
- [37] T. Alm *et al.*, *Phys. Lett. B* 346:233 (1995).
- [38] W. Reisdorf and H.G. Ritter, *Ann. Rev. Nucl. Part. Science* 47:663 (1997).
- [39] J. Hubele *et al.*, *Phys. Rev. C* 46:R1577 (1992).
- [40] U. Milkau *et al.*, *Phys. Rev. C* 44:R1242 (1991).
- [41] For a recent review see D. Ardouin, *Int. J. Mod. Phys. E* 6:391 (1997).
- [42] S. Fritz, PhD thesis, Universität Frankfurt (1997).
- [43] S. Pratt and M.B. Tsang, *Phys. Rev. C* 36:2390 (1987).
- [44] J. Gosset *et al.*, *Phys. Rev. C* 16:629 (1977).
- [45] D.H. Boal and J.C. Shillcock, *Phys. Rev. C* 33:549 (1986).